


Article Information

Article Type:	Research Article
Journal Title:	Molecular Crystals and Liquid Crystals
Publisher:	Taylor & Francis
DOI Number:	10.1080/15421406.2024.2358731
Volume Number:	0
Issue Number:	0
First Page:	1
Last Page:	11
Copyright:	© 2024 Taylor & Francis Group, LLC
	

Electric field effect on the absorption coefficient of hemispherical quantum dots

Left running head: V. A. HOLOVATSKY ET AL.

Short title : Molecular Crystals and Liquid Crystals

AQ0

 V. A. Holovatsky^a,  I. V. Holovatsky^b and  C. A. Duque^c

^aDepartment of Thermoelectricity and Medical Physics, Chernivtsi National University after Yuriy Fed'kovich, Chernivtsi, Ukraine;

^bDepartment of Information Technologies and Computer Physics, Chernivtsi National University after Yuriy Fed'kovich, Chernivtsi, Ukraine;

^cGrupo de Materia Condensada-UdeA, Facultad de Ciencias Exactas y Naturales, Instituto de Física, Universidad de Antioquia, Medellín, Colombia

Corresponding Author

CONTACT V. A. Holovatsky v.holovatsky@chnu.edu.ua Department of Thermoelectricity and Medical Physics, Chernivtsi National University after Yuriy Fed'kovich, Chernivtsi, Ukraine.

Abstract

This study presents a simple model within the effective mass approximation to describe the effect of an external electric field on the energy structure and wave functions of quasiparticles in type II hemispherical quantum dots. The case of an electric field perpendicular to the base of a hemispherical quantum dot is considered. The solutions of the Schrödinger equation were obtained by two methods: finite element method and the matrix method. The last method allowed to determine the partial contribution of the basic states in the new states of quasiparticles obtained as a result of the action of an electric field.

KEYWORDS

finite element method; hemispherical quantum dot; matrix method; optical absorption; oscillators strength; type II core/shell QD

Introduction

In recent years, semiconductor quantum dots different forms have attracted significant interest in scientific research. These nanoscale particles possess unique properties and open up a wide range of possibilities for improving existing and developing new optoelectronic devices [1, 2]. Quantum size effects play a key role in the optoelectronic properties of nanoparticles, as the absorption and emission energies depend on their sizes. Besides size, the geometric shape of quantum dots is also a crucial characteristic that significantly influences their electronic structure and physical properties. Depending on the growth methods, quantum dots can assume various shapes. In addition to spherical and cylindrical, which are the most studied, modern technologies allow growing pyramidal, elliptical, lens-like, semi-spheroid and dome-shaped quantum dots [3–6].

Quantum dots can have a complex internal structure, which allows obtaining the energy spectrum and wave functions of quasiparticles required for practical applications. In recent years, a new paradigm in the modeling of nanostructures, known as wave function engineering, has appeared [7–11]. This approach enables the design of nanostructures with high light absorption and emission efficiency, increased quantum yields, emission wavelengths. Multilayer quantum dots are used to achieve desired optical characteristics, including optical absorption and emission [10–13]. The simplest of these are core-shell quantum dots, which can be classified into different types based on the relative positions of the bandgaps of the core and shell materials. In type-II quantum dots, electrons and holes are spatially separated in different potential wells, reducing the effective bandgap and shifting absorption energies toward longer wavelengths. This separation also decreases the probability of radiative recombination processes, enhancing the efficiency of photovoltaic conversion.

The simplest nanostructures for theoretical investigations are those for which exact solutions of the Schrödinger equation exist. For other cases, various approximation methods or numerical solutions of partial differential equations are used, such as finite difference or finite element methods. The studies [14, 15] investigate the magnetic and electric field effects on the optical properties of spherical core-shell Type II quantum dots using wave function expansion based on an orthonormal basis of exact solutions of the Schrödinger equation. The dependencies of the oscillator strength and the quantum energy transition on electric field strength and magnetic field induction are calculated. However, these studies have been performed for spherical quantum dots grown by colloidal chemistry methods. In the case of self-organized QDs on a flat surface, their shape is non-spherical but can be approximated as hemispherical. In the case of hemispherical quantum dots (HSQD) with infinite potential at the planar boundary, using the effective mass approximation and rectangular potential barrier, one can obtain wave functions in analytical form and exact energy spectra [16, 17]. This makes it possible to obtain approximate solutions for many more complicated problems. In previous research [18], the authors investigated the electronic states in lens-shaped quantum dots based on the wave functions of electrons in semi-spherical quantum dots with infinite potential barriers on all boundaries. In another study [19], the influence of a periodic electric field on the energy spectrum of HSQD was explored. The Zeeman splitting in hemispherical quantum dots has been studied by Lopez Gondar and others [20] on the orthonormal wave functions obtained for an electron in HSQD without a magnetic field.

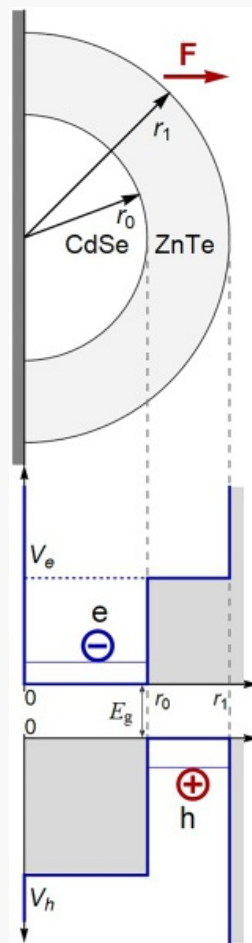
In this paper, we investigate the effect of a uniform electric field on the electron and hole states in the core-shell of a type II HSQD. The energy spectrum of quasiparticles and their distribution in the nanostructure are

obtained using a single-particle Schrödinger equation solved by the matrix method. To perform these calculations, the quasiparticle wave functions are represented as expansions in an orthonormal basis of exact solutions of the Schrödinger equation in the absence of external fields. This orthonormal basis is constructed based on a linear combination of Bessel functions satisfying the boundary conditions of the investigated core-shell quantum dot. The obtained results are compared with result finite element method via the 2D axis-symmetric module of COMSOL-Multiphysics software.

Theoretical framework

The hemispherical quantum dot studied in this paper consists of a core (CdSe) and a hemispherical layer (ZnTe). The radius of the core is r_0 , the outer radius of the spherical layer is r_1 . The geometric scheme and scheme of the potential profile of the conduction band and valence band are shown in Figure 1.

Figure 1. Geometric and potential scheme of HSQD.



The Schrödinger equation for an electron has the following form

$$-\frac{\hbar^2}{2} \vec{\nabla} \frac{1}{\mu_{e,h}(r)} \vec{\nabla} \Phi_{nlm}^{e,h}(\vec{r}) + U_{e,h}(r, \theta) \Phi_{nlm}^{e,h}(\vec{r}) = E_{nl}^{e,h} \Phi_{nlm}^{e,h}(\vec{r}),$$

where

$$\mu_{e,h}(r) = \mu_0 \begin{cases} m_0^{e,h}, & r \leq r_0 \\ m_1^{e,h}, & r_0 < r \leq r_1 \end{cases},$$

μ_0 – free electron mass, $U_{e,h}(r, \theta) = U'_{e,h}(r) + U''(\theta)$,

$$U''(\theta) = \begin{cases} 0, & 0 < \theta \leq \pi/2 \\ \infty, & \pi/2 < \theta < \pi \end{cases}$$

$$U'_{e(h)}(r, \theta) = \begin{cases} 0(V_h), & r \leq r_0, \\ V_e(0), & r_0 < r \leq r_1, \\ \infty, & r > r_1. \end{cases}$$

We find solutions of [Equation \(1\)](#) as for the corresponding spherical quantum dot in the form

$\Phi_{nlm}^{e,h}(\vec{r}) = R_{nl}^{e,h}(r)Y_{lm}(\theta, \varphi)$, but we choose those solutions which satisfy the boundary condition for HSQD

$$Y\left(\frac{\pi}{2}, \varphi\right) = 0.$$

Considering $Y(\theta, \varphi) = A P_l^{|m|}(\cos\theta)e^{im\varphi}$, where $P_l^{|m|}(x)$ – associated Legendre polynomials, condition (5) is fulfilled for such values of l and m for which $P_l^{|m|}(0) = 0$. As follows from the property of associated Legendre polynomials $P_l^{|m|}(x) = (-1)^{l+|m|} P_l^{|m|}(x)$, the boundary condition is fulfilled when $l + |m| = 2p + 1$, where $|m| < l$, $p = 1, 2, \dots$. The radial part of the wave function of each quasiparticle in the regions where the energy of the quasiparticle is greater than the potential energy $E_{nl}^{e,h} > V_{h,e}$ is obtained in the form of a linear combination of spherical Bessel functions of the 1st and 2nd kind

$$R_{nl}^{e,h}(r) = A j_l(k_n^{e,h} r) + B n_l(k_n^{e,h} r),$$

where

$$k_n^{e,h} = \frac{1}{\hbar} \sqrt{2\mu_{e,h} (E_{nl}^{e,h} - V_{e,h})}.$$

In those regions where $E_{nl}^{e,h} < V_{h,e}$, in order to avoid complex numbers, appropriate modified spherical Bessel functions are used. The unknown coefficients A, B and $k_n^{e,h}$ are obtained from the boundary conditions

$$\left. \begin{aligned} R_{nl}^{(i)}(r_i) &= R_{nl}^{(i+1)}(r_i) \\ \frac{1}{m_i} \frac{dR_{nl}^{(i)}(r)}{dr} \Big|_{r=r_i} &= \frac{1}{m_{i+1}} \frac{dR_{nl}^{(i+1)}(r)}{dr} \Big|_{r=r_i} \end{aligned} \right\}, i = 0, 1$$

and normalization conditions that takes into account the hemispherical shape of the quantum dot.

In order to calculate the influence of external electric fields parallel to the Oz axis on the energy spectrum and wave functions of electron and hole localized in HSQD, it is necessary to solve the following Schrödinger equation

$$H^{e,h} \psi_{jm}^{e,h}(\vec{r}) = \tilde{E}_{jm}^{e,h} \psi_{jm}^{e,h}(\vec{r})$$

with the Hamiltonian

$$H^{e,h} = -\frac{\hbar^2}{2} \nabla^2 \frac{1}{m^{e,h}(r)} \nabla^2 \pm eFrcos \theta + U^{e,h}(r),$$

where F is the electric field strength. When external fields are applied to the system, Schrödinger equation (1) cannot be solved analytically. Therefore, the method of the electron wave functions expansion is used.

Electron wave function $\Psi_{jm}(\vec{r})$ has the form

$$\Psi_{jlm}(\vec{r}) = \sum_n \sum_l c_{nl}^{jm} \Phi_{nlm}(\vec{r}).$$

The wave functions expanded coefficients c_{nl}^{jm} and energy spectrum $E_{jlm}^{e,h}$ are obtained from secular equation by the diagonalization method. Using the wave function (11) the oscillator strengths of the interband quantum transitions defines the strength of absorption lines, and can be obtained via the expression [10]

$$F_{f-i} \sim \int_{\Omega} \psi_{jlm}^e(\vec{r}_e) \psi_{jlm}^{h*}(\vec{r}_h) \delta(\vec{r}_e - \vec{r}_h) d\vec{r}_e d\vec{r}_h,$$

The selection rules for interband quantum transitions in HSQDs differ from those in spherical nanostructures. Wave functions with different values of the orbital quantum number are no longer orthogonal in the region of the hemispherical quantum dot. The selection rules become the same as for cylindrical systems

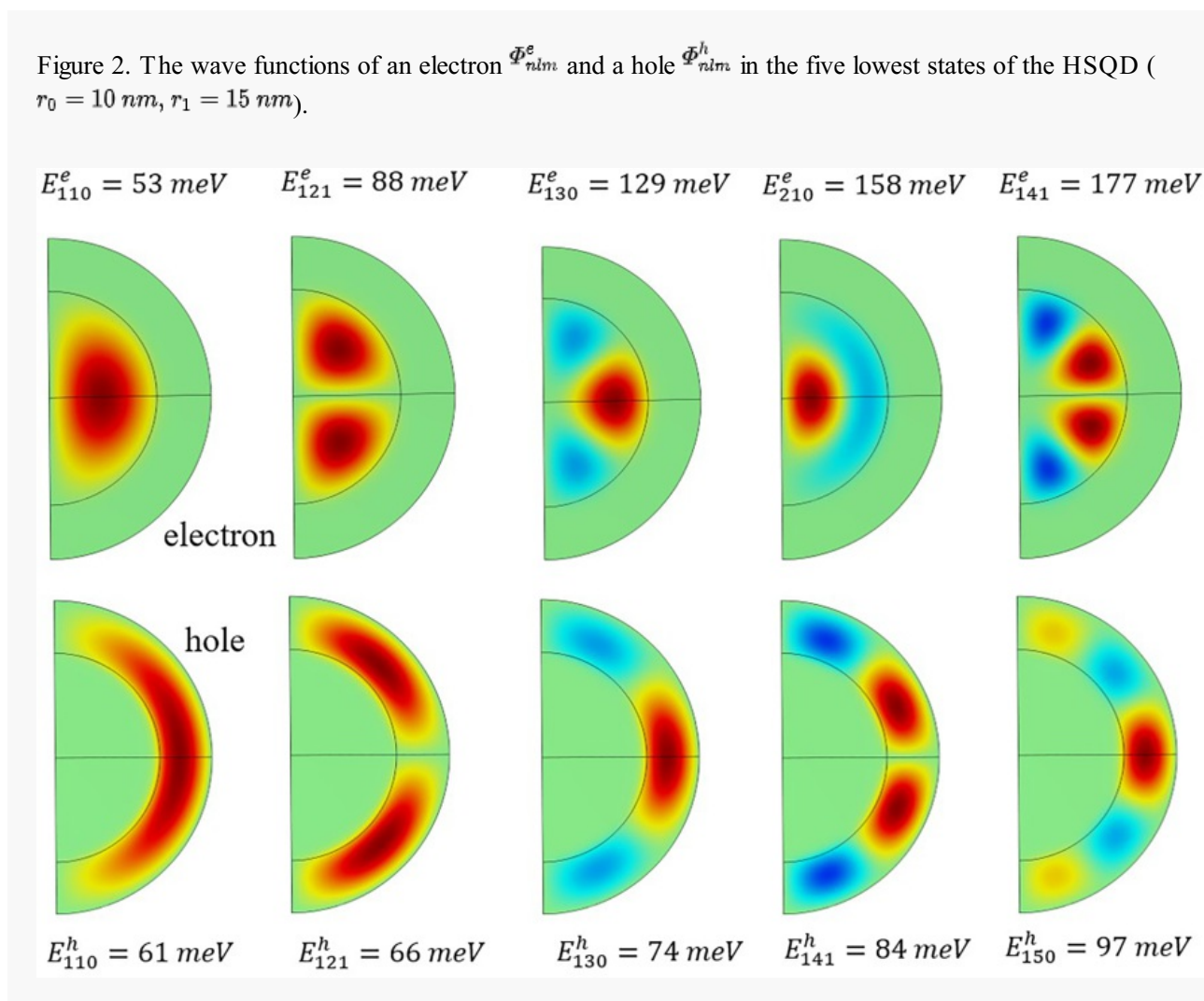
$$\int_0^{2\pi} \int_0^{\pi/2} Y_{l'm'}^* Y_{lm} \sin \theta d\theta d\varphi \sim \delta_{m'm}.$$

Analysis and discussion of results

The computer calculations have been done for HSQD CdSe/ZnTe with following physical parameters: CdSe: $m_0^e = 0.13$, $m_0^h = 0.45$, $E_g^{CdSe} = 1.75$ eV; ZnTe: $m_1^e = 0.15$, $m_0^h = 0.2$, $E_g^{ZnTe} = 2.2$ eV. $V_e = 1.27$ eV, $V_h = 0.84$ eV – potential barrier for an electron and hole at the CdSe/ZnTe heterojunction.

The energy spectrum of an electron and a hole in an HSQD in the absence of external fields consists of solutions of the Schrödinger equation (1) that satisfy the boundary condition (5), i.e., of the energies of states for which the sum of the orbital and magnetic quantum numbers is an odd number $l + |m| = 2p + 1$, where $p = 1, 2, \dots$. Therefore, in the energy spectrum of the HSQD there are states with an odd value of $l = 1, 3, \dots$, but an even value of $m = 0, \pm 2, \dots$, as well as states with an even value of $l = 2, 4, \dots$, but odd value of $m = \pm 1, \pm 3, \dots$. The ground states of an electron and hole are states with $l = 1, m = 0$. The energies of the excited states with $m \neq 0$ are doubly degenerate for the magnetic quantum number sign. The energy spectrum of the HSQD contains the same energies as the corresponding spherical quantum dot except for the spherically symmetric s-states ($n = 1, 2, 3 \dots; l = 0$), which do not satisfy condition (5).

The wave functions of an electron Φ_{nlm}^e and a hole Φ_{nlm}^h in HSQD CdSe/ZnTe at $r_0 = 10 \text{ nm}$, $r_1 = 15 \text{ nm}$ in several lowest states are shown in Figure 2.



It can be seen from the figure that the electron is localized in the core of the HSQD, and the hole is in the spherical shell, and the overlap of the wave functions occurs due to the tunneling effect in the narrow region near core-shell heterojunction.

The wave functions $\Phi_{nim}^{e,h}(\vec{r})$ form an orthonormal basis for calculations the wave functions $\psi_{jm}^{e,h}(\vec{r})$ and the energy spectrum $\tilde{E}_{jm}^{e,h}$ of electrons and holes in HSQD placed in an external electric field. Since, in the case of the electric field effect, the magnetic quantum number remains a "good" quantum number, the decomposition occurs only in states with different values of the quantum numbers n and l . The quantum number j indicates the number of the new state of the quasiparticle at a given quantum number m .

Calculations of energies and wave functions were performed by two methods: the diagonalization method and finite element method (FEM) in COMSOL. In expansion (11), about 10 terms were taken into account, which ensured the accuracy of the calculation of about 0.1-0.4%. To demonstrate the convergence of the results, obtained by different methods, Table 1 shows the energies of the ground states of the electron E_{10}^e and the hole E_{10}^h in the QD at different values of electric field.

Note: The table layout displayed in 'Edit' view is not how it will appear in the printed/pdf version. This html display is to enable content corrections to the table. To preview the printed/pdf presentation of the table, please view the 'PDF' tab.

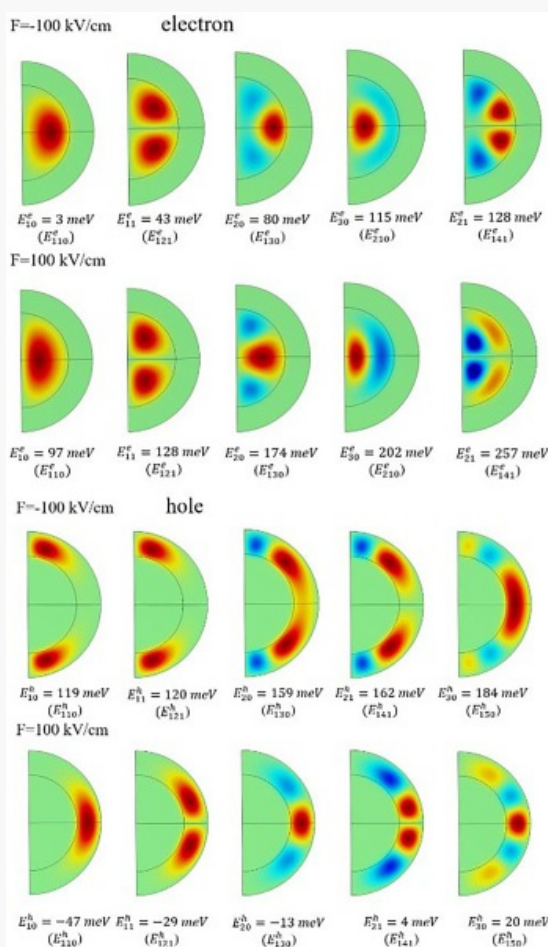
Table 1. Comparison of the ground state energies of an electron E_{10}^e and a hole E_{10}^h obtained using both the diagonalization method and FEM in COMSOL software at different values of electric field strength.

Methods	$E_{jm}^{e,h}$	F, kV/cm						
		-100	-50	-25	0	25	50	100
Diagonalization (matrix)	E_{10}^e , meV	3.146	29.18	41.52	53.41	64.87	75.92	96.86
	E_{10}^h , meV	119.4	95.57	80.70	60.90	36.11	9.215	-46.90
FEM (COMSOL)	E_{10}^e , meV	3.181	29.21	41.55	53.45	64.91	75.96	96.89
	E_{10}^h , meV	118.9	95.59	80.77	60.96	36.17	9.273	-46.84

Place the cursor position on table column and click 'Add New' to add table footnote.

Figure 3 show the wave functions of an electron $\psi_{jm}^e(\vec{r})$ and a hole $\psi_{jm}^h(\vec{r})$ in the five lowest states at $F = \pm 100 \text{ kV/cm}$, which demonstrate the distribution of quasiparticles in the nanostructure. It can be seen from Figure 3 that the electric field displaces both quasiparticles in different directions, but at the same time, the wave functions of the hole, which is localized in the shell of the nanostructure, deform more strongly. The topology of the hole wave function under influence of an electric field directed to the plane boundary HSQD changes from quantum dot to quantum ring, both for the ground and excited states. A similar effect was observed in the results of the study self-organized QD type II InAs/GaAsSb [19].

Figure 3. The wave functions of an electron ψ_{jm}^e and a hole ψ_{jm}^h in the five lowest states at $F = \pm 100 \text{ kV/cm}$.



An interesting effect of the electric field is observed for the wave functions of the hole, which shifts it in the direction of the planar heterojunction. The hole distribution in the states $\psi_{10}^h(\vec{r})$ and $\psi_{11}^h(\vec{r})$ at

$F = -100 \text{ kV/cm}$ and the values E_{10}^h and E_{11}^h become similar. With a stronger electric field, this situation is also observed for the next pairs $\psi_{20}^h(\vec{r}')$, $\psi_{21}^h(\vec{r}')$ and others.

The dependences of quasiparticle energies on the value and direction of the electric field are shown in Figure 4. Most of the energy levels of electrons and holes are nearly linearly dependent on the electric field strength. But the dependences of several hole energy levels in the case of a negative electric field are nonlinear. Among them, the largest nonlinearity is observed in the dependences of the state with $j = 1$ – lowest states at each value of the magnetic quantum number m and also other states, which are formed from states $l = m + 1$.

Figure 4. Dependence of the energy spectrum of electrons and holes in the HSQD on the electric field strength ($m = 0$ – first column, $|m| = 1, 2$ – second column).

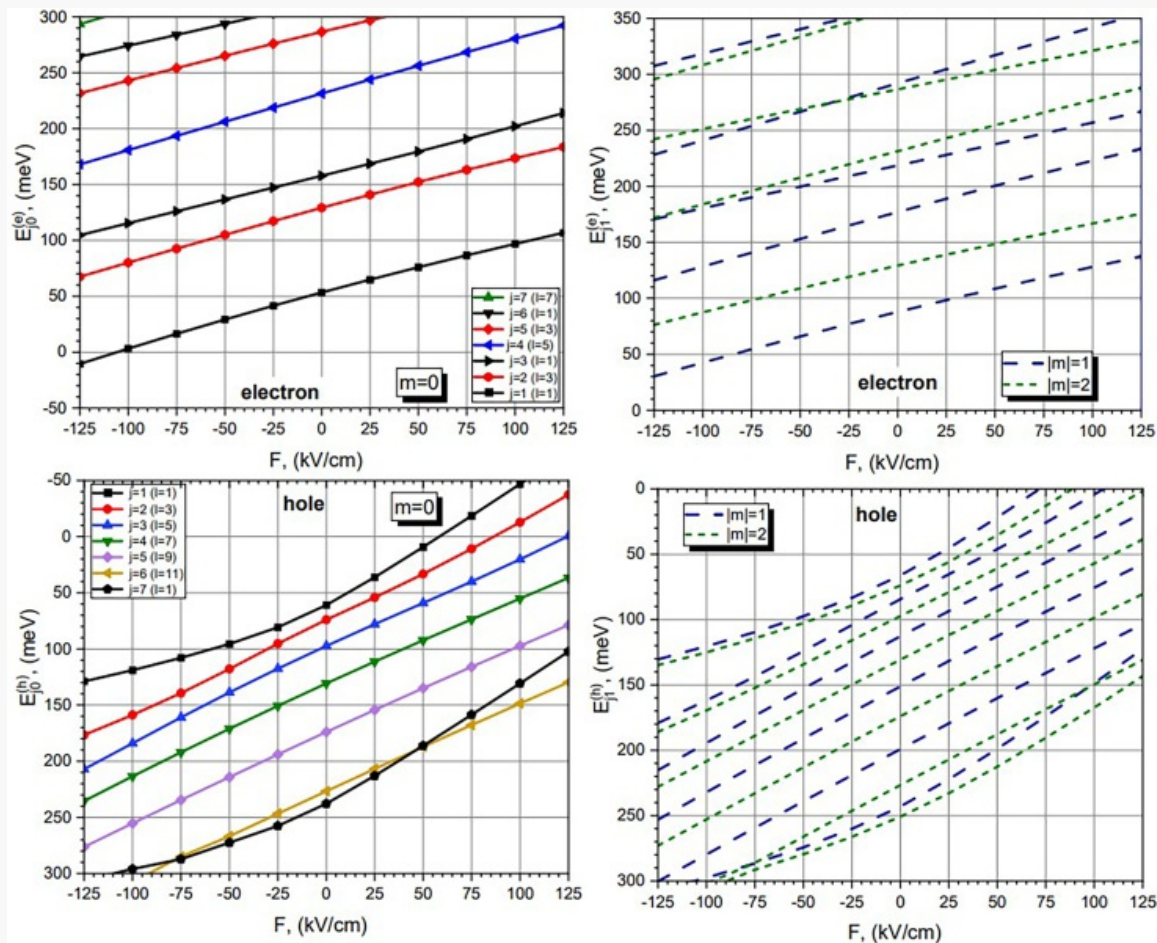
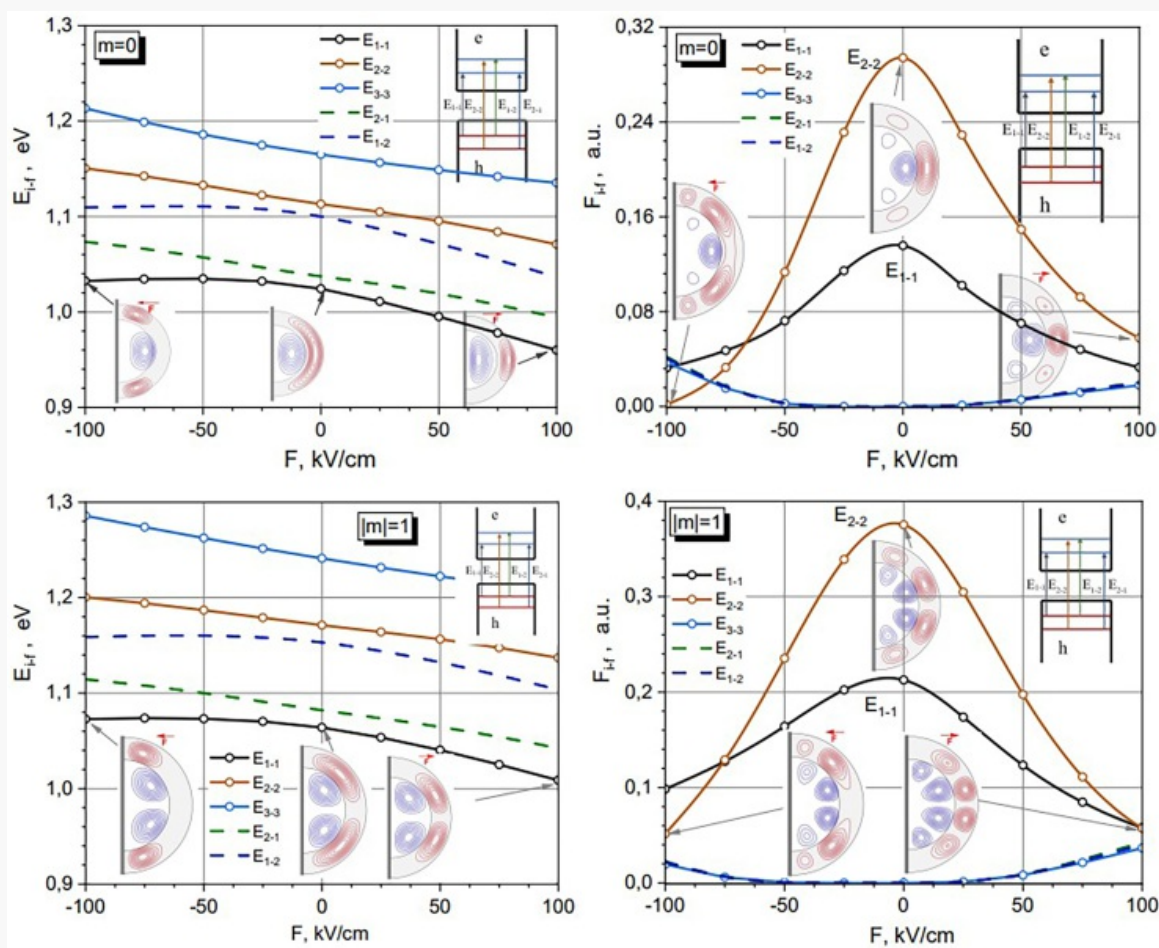


Figure 5 shows the dependence of the energies and oscillator strength of the several interband quantum

transitions on the electric field. These dependencies, in contrast to spherical quantum dots, have an asymmetric shape. The energy of the quantum transition between the ground states of an electron and a hole rapidly decreases with an increase in the intensity of the electric field oriented in the direction of quantum dot growth. However, at the opposite direction of the electric field effect is significantly weaker. This result qualitatively coincides with the result obtained by J. M. Llorens and others for self-organized QD type II InAs/GaAsSb [21].

Figure 5. Dependencies of the energy transitions (on the left) and oscillator strength (on the right) on the electric field strength ($m = 0$ – top row; $|m| = 1$ – bottom row).



In the absence of an electric field, the oscillator strength of the quantum transition between ground states of quasiparticles $\psi_{10}^{e,h}$ ($j = 1, m = 0$) is weaker than between excited states $\psi_{20}^{e,h}$, $\psi_{11}^{e,h}$ and $\psi_{21}^{e,h}$. For mixed quantum transitions between electron and hole states with different quantum numbers j , the oscillator strength is zero.

However, under the influence of an electric field, the oscillator strength for the first quantum transitions decreases, while it increases for mixed quantum transitions.

Conclusions

In this paper, we have investigated the electric field effect on the energy spectrum and wave functions of an electron and a hole in the hemispherical quantum dots II type CdSe/ZnTe. An electron and a hole in such a nanostructure are spatially separated, and the electric field affects their energy spectrum and distribution in the HSQD in different ways. The results of the study show that the optical properties of hemispherical quantum dots combine the properties of spherical and cylindrical nanostructure, and also have asymmetry in relation to the direction of the electric field.

HSQD does not have spherical symmetry, but the wave functions of quasiparticles in such a nanostructure contain spherical functions. In the absence of an electric field, the quantum states of quasiparticles are characterized by an orbital quantum number. As a result, the rules for selecting interband quantum transitions in HSQDs are the same as for spherical nanosystems, that is, transitions between states of quasiparticles with different values of the orbital quantum number are forbidden. However, the probability of such mixed quantum transitions increases under the influence of an electric field. Unlike spherical quantum dots, the energy of quantum transitions in HSQDs depends on the direction of the electric field.

















Disclosure statement AQ1

No potential conflict of interest was reported by the author(s).


Note: this Edit/html view does not display references as per your journal style. There is no need to correct this. The content is correct and it will be converted to your journal style in the published version.

References

- 1 D. Vasudevan *et al.*, *J. Alloy. Compd.* **636**, 395 (2015). Doi: 10.1016/j.jallcom.2015.02.102. ↑
- 2 R. G. Chaudhuri and S. Paria, *Chem. Rev.* **112** (4), 2373 (2012). Doi: 10.1021/cr100449n. ↑
- 3 E. C. Niculescu, *Phys. E.* **63**, 105 (2014). Doi: 10.1016/j.physe.2014.05.012. ↑
- 4 M. Shahzadeh and M. Sabaeian, *AIP Adv.* **4**, 6 (2014). Doi: 10.1063/1.4885135. ↑
- 5 L. Aderras *et al.*, *Phys. Status Solidi Basic Res.* **254** (10), 1700144 (2017). Doi: 10.1002/pssb.201700144. ↑

- 6 C. Heyn *et al.*, *Nanomaterials* **13** (5), 857 (2023). Doi: 10.3390/nano13050857. 
- 7 H. Zhu *et al.*, *J. Am. Chem. Soc.* **133** (22), 8762 (2011). Doi: 10.1021/ja202752s. 
- 8 L. Rammohan *et al.*, in *Handbook of Nanostructured Materials and Nanotechnology* (Elsevier, 2000), Vol. 2, pp. 707–739. Doi: 10.1016/B978-012513760-7/50031-9. 
- 9 F. Koç and M. Sahin, *Appl. Phys. A.* **125** (10), 705 (2019). Doi: 10.1007/s00339-019-3000-3. 
- 10 V. Holovatsky and I. Frankiv, *J. Optoelectron. Adv. Mater.* **15** (1-2), 88–93 (2013). 
- 11 R. Y. Leshko *et al.*, *Micro and Nanostructures* **181**, 207615 (2023). Doi: 10.1016/j.micrna.2023.207615. 
- 12 M. Chubrei *et al.*, *Philos. Mag.* **101** (24), 2614 (2021). Doi: 10.1080/14786435.2021.1979267. 
- 13 V. Holovatsky *et al.*, *Phys. Chem. Solid State* **4** (4), 630 (2021). Doi: 10.15330/pcss.22.4.630-637. 
- 14 V. Holovatsky *et al.*, *Appl. Nanosci.* **13** (11), 7125 (2023). Doi: 10.1007/s13204-023-02877-4. 
- 15 V. Holovatsky *et al.*, *Thin Solid Films* **747**, 139142 (2022). Doi: 10.1016/j.tsf.2022.139142. 
- 16 N. Mohajer *et al.*, *Phys. B. Condens. Matter.* **497**, 51 (2016). Doi: 10.1016/j.physb.2016.05.028. 
- 17 S. Wu, *Chin. Phys. B.* **30** (5), 053201 (2021). Doi: 10.1088/1674-1056/abd472. 
- 18 A. H. Rodríguez *et al.*, *Phys. Rev. B.* **63** (12), 1253191 (2001). Doi: 10.1103/physrevb.63.125319. 
- 19 A. H. Rodríguez *et al.*, *Phys. Status Solidi* **242** (9), 1820 (2005). Doi: 10.1002/pssb.200461710. 
- 20 J. Lopez Gondar *et al.*, *Phys. Status Solidi* **230** (2), 437 (2002). Doi: 10.1002/1521-3951(200204)230:2<437:AID-PSSB437>3.0.CO;2-I. 
- 21 J. M. Llorens *et al.*, *Appl. Phys. Lett.* **107**, 18 (2015). Doi: 10.1063/1.4934841. 

Author Query

1. **Query [AQ0]** : Please review the table of contributors below and confirm that the first and last names are structured correctly and that the authors are listed in the correct order of contribution. This check is to ensure that your names will appear correctly online and when the article is indexed. 

Sequence	Prefix	Given name(s)	Surname	Suffix
1		V. A.	Holovatsky	
2		I. V.	Holovatskyi	
3		C. A.	Duque	

Response by Author: "Ok"

2. **Query [AQ1]** : The disclosure statement has been inserted. Please correct if this is inaccurate. 

Response by Author: "Ok"

3. **Query [AQ2]** : Please note that the ORCID section has been created from information supplied with your manuscript submission/CATS. Please correct if this is inaccurate. 

Response by Author: "Ok"